Study on the mechanism of the squeeze-strengthen effect in magnetorheological fluids

X. Z. Zhang, X. L. Gong, and P. Q. Zhang
CAS Key Laboratory of Mechanical Behavior and Design of Materials, Department of Mechanics and Mechanical Engineering, University of Science and Technology of China, Hefei, Anhui 230027, China

Q. M. Wang
Department of Precision Machinery and Precision Instrumentation, University of Science and Technology of China, Hefei, Anhui 230027, China

(Received 21 November 2003; accepted 25 May 2004)

Current magnetorheological (MR) fluids have the limitation that their yield stresses are not strong enough to meet some industrial requirements. X. Táng, X. Zhang, and R. Tao [J. App. Phys **87**, 2634 (2000)] proposed a method to achieve high-efficiency MR fluids by study of squeeze-strengthen effect. But there is little report on its mechanism. This paper aims to investigate this effect through experimental and theoretical approaches. For this purpose, an apparatus is designed to experimentally study the mechanism of this squeeze-strengthen effect. Taking account of a modified magnetic dipole model and the friction effect, a semiempirical model is proposed to explain this effect. In addition, this model is expected to study the squeeze-strengthen effect in electrorheological fluids. © *2004 American Institute of Physics*. [DOI: 10.1063/1.1773379]

I. INTRODUCTION

As a kind of controllable material, magnetorheological (MR) fluids have been widely used in various devices, such as MR dampers and MR clutches.[1–4] MR fluids can reversibly change their states between free-flowing, linear viscous liquids and semisolids having controllable yield strength within milliseconds after a magnetic field is turned on or off. This promising feature makes it to be a simple, quiet, rapid interface between electronic control system and mechanical system. But the yield stresses of current MR fluids are not strong enough for some requirements of industry.[5]

Usually MR fluids are composed of magnetizable particles (such as iron particles) and nonmagnetic matrix. When MR fluids are exposed to a magnetic field, the magnetizable particles acquire a dipole moment aligned with the applied field that causes the particles to form linear chains parallel to the field. This phenomenon results in the solidification of the suspension. Only the applied external shear force is larger than the yield stress, the suspension can flow again. The yield stress increases steadily with increasing the magnetic flux density, but the ultimate strength of the MR fluids depends on the square of the saturation magnetization strength of the magnetizable particles.[1–3] Therefore, the key point to enhance the yield stress of MR fluids is to choose a particle material with large saturation magnetization.[1–3] The widely used particle material is simply pure iron with a high saturation magnetization 2.1 T. MR fluids with powders of carbonyl iron can achieve the yield stress of about 100 kPa. In addition, the yield stress can also be improved by increasing the volume fraction of magnetizable particles. But the volume fraction has an upper limit. Ginder and Davis[3] used a finite-element technique to study the effects of magnetic nonlinearity and saturation on the shear stress of magnetorheological fluids. They found that the local saturation of the particle magnetization determined the shear stress over a wide range of magnetic inductions and predicted that the yield stress of an iron-based MR fluid at 50% volume fraction could reach a maximum of 210 kPa.

To attain higher yield stress, Táng *et al.*[5] compressed MR fluids along the field direction when a magnetic field was applied. They reported that the yield stress of MR fluids could be increased ten times, which was strong enough for many industry requirements such as flexible fixtures. They gave a tentative explanation that the particle chains in the MR fluids were pushed together to form thick columns and the yield stress of MR fluids was consequently improved by changing their microstructure. But traditional magnetic dipole model cannot explain the fact that the static yield stress of MR fluids exceeding 800 kPa. Because the reason for this is that this model is used to deal with the condition when the distance between the particles is much larger than their size. In addition, it is also inadequate to explain the squeeze-strengthen effect by the theory of thick particle column.

In this paper, an apparatus is designed to study the mechanism of the squeeze-strengthen effect in MR fluids. The theoretical approach by modifying the traditional magnetic dipole model using local field theory and tribology indicates that the MR effect can be improved greatly when the magnetic particles are pushed closely. This model is also verified by experiments.

II. EXPERIMENTAL EQUIPMENT

The used MR fluids contain 46% volume fraction carbonyl iron particles, which have an average diameter of 3–5 μm. These particles are suspended in silicon oil. The equipmental setup is shown in Fig. 1. MR fluids are contained in a copper container, which can adjust the distribution of magnetic field and let most of the magnetic flux can pass through the MR fluids. The magnetic field is generated by a coil by adjusting the electric current density. A Tesla

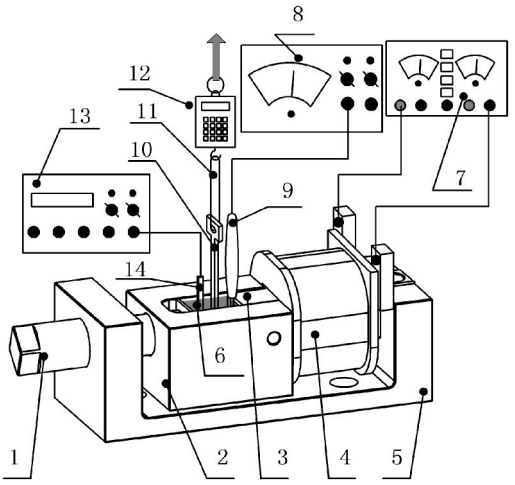

FIG. 1. Experimental setup. 1, iron bolt; 2, container (copper) 3, iron bar; 4, coil; 5, base (iron) 6, MR fluids; 7, dc power supply; 8, tesla gauge; 9, tesal probe; 10, thin aluminum slice (or iron slice) 11, brass wire; 12, tensile gauge; 13, strain gauge; 14, pressure sensor.

gauge is set to measure the magnetic flux density. The Tesla probe is inserted into the MR fluids to measure the actual magnetic field in the sample. Because of demagnetization effects, the flux density measured by the probe in the MR fluids will be lower than the real flux density in vacuum. But this phenomenon has little influence on the relative flux density. Measurement of a series of measurements in both ends of the sample indicates that the magnetic flux density in the sample is almost the same, which demonstrates that the magnetic field is uniform. The base of the equipment setup is made of soft iron and all the parts are mounted on it. One side of the container is blocked with soft iron bar and electromagnet. The other side is a soft iron block and a bolt that are used to compress MR fluids along the field direction. The compression stress in MR fluids is measured by a pressure sensor. The base, bolt, MR fluids, and electromagnet form a close electromagnetic path. A thin metal slice (aluminum or iron slice) is plugged into the MR fluids to measure the squeeze-strengthen effect. This slice is pulled and the force is measured by a tensile gauge. In other words, pull the slice until the structure is broken, and the yield stress can be measured.

III. EXPERIMENTAL RESULTS

By using this setup, yield stress of MR fluids in different magnetic flux density (0–350 mT) and compression stress (0–10 MPa) are obtained. Figure 2 shows experimental results of MR yield stresses under various compression pressures and different field strengths when an aluminum slice is used. The measured data are marked by diamond and the data are fit to a three-dimensional (3D) surface. To explain the results clearly, some data are extracted and form two-dimensional (2D) profiles as shown in Fig. 3. When there is no compression, yield stress increases linearly as the flux density increases. At low compression stresses of 2.0 MPa and 4.0 MPa, the curve shows the same tendency. With the compression stress increasing, the curve of the yield stress versus flux density goes upward. For example, at the compression stress of 6.3 MPa, the yield stress increases steadily at low flux density, then increases sharply above a certain flux density. Further increasing the compression stress, e.g., 9.9 MPa, the yield stress becomes stable after an initial quick increase stage. These results are due to the squeeze-strengthen effect. At low-compression stress (include no compression) stage, there is no particle saturation, thus the yield stress increases linearly with increasing field strength. With the pressure load increasing, the distance of particles becomes shorter, the interaction of dipoles becomes stronger, and therefore the yield stress increases because the formed chain structure is difficult to be broken. The higher the compression stress is, the more obvious the squeeze-strengthen effect is. Thus, the saturation at high load is more easily observed than that at low load, which are reflected in Fig. 2. Similarly, the squeeze-strengthen effect is summarized in Fig. 4 and 5 when an iron slice is used to replace the aluminum one. Except the same increasing tendency, the yield stress with an iron slice is bigger than that that with an aluminum slice. Figure 6 shows the comparison of yield stress with the iron slice and with the aluminum. Both of these two cases are measured at the same magnetic flux density of 275 mT. At the same compression stress, the yield stress with the iron slice is much larger than that with the aluminum slice. This difference is because of the wall effect,[6] which also results in different structure-break modes. For the aluminum slice case, structure-break happens between the slice and the MR fluid; while for the iron slice case it hap-

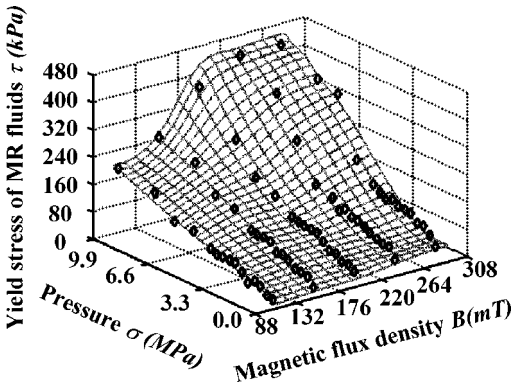

FIG. 2. 3D experimental result surface of yield stress, compression stress, and magnetic flux density (measured by aluminum slice).

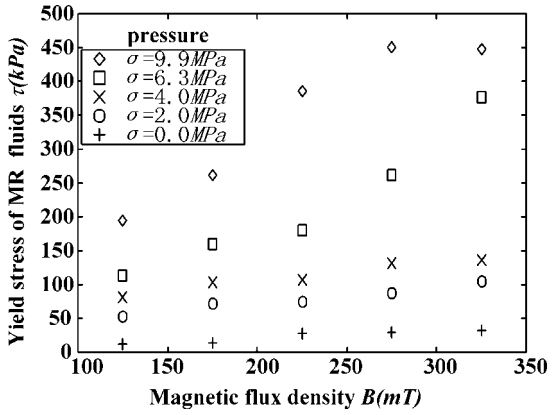

FIG. 3. 2D experimental results (measured by aluminum slice).

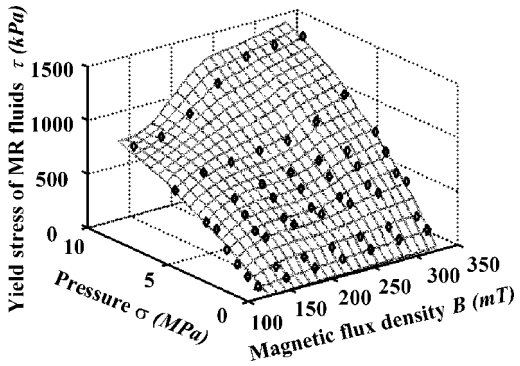

FIG. 4. 3D experimental result surface of yield stress, compression stress, and magnetic flux density (measured by iron slice).

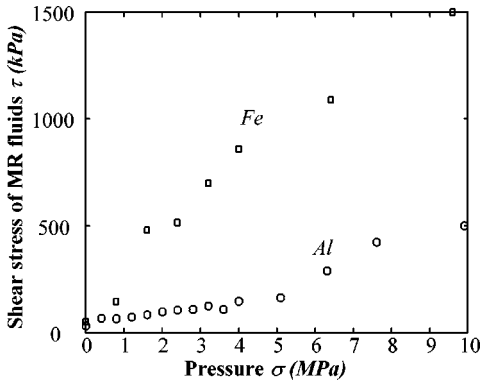

FIG. 6. Comparison between different work pieces (B=275 mT).

pens in MR fluids. This phenomenon means that the binding stress between the iron slice and MR fluids is larger than the yield stress in MR fluids, while the binding stress between aluminum slice and MR fluids is less than the yield stress in MR fluids.

According to the wall effect[6] analysis, additional force between a particle and a wall can be approximated by the interaction between the magnetic moment **m** of the particle and its image $\mathbf{m}_{\text{im}}$ in the wall, whose amplitude $\mathbf{m}_{\text{im}}$ is equal to

$$m_{\text{im}} = \frac{m(\mu_w - \mu_e)}{(\mu_w + \mu_e)}, \tag{1}$$

where μ_w is the magnetic permeability of the wall and μ_e the permeability of the suspending liquid. When an iron slice is used, its permeability is very large compared to unity, the magnetic dipole induced by the field and its image is parallel resulting in an attractive force. But when an aluminum slice is used, its permeability is very close to the oil, so from Eq. (1), there is no additional force between magnetizable particles and the wall. Even if the roughness of iron or aluminum slice are quite identical, in the first case the particles are pushed against the defects of the wall where they become trapped, whereas in the other case they can roll more easily over small bumps. From this result, if MR fluids are applied to flexible fixtures, ferromagnetic materials are easier to be fixed than other materials. Moreover, the yield stress measured by aluminum slice is only the force between the slice and the MR fluid. The yield stress measured by iron slice is the real yield stress of MR fluids. Táng *et al.*[5] used an aluminum slice to measure the structure-enhanced yield stress and got the yield stress of 800 kPa, 10 times the yield stress without compression. For our experiment with the iron slice, a much stronger squeeze-strengthen effect is observed. For example, at the flux density of 325 mT, and compression stress of 9.6 MPa, the yield stress can reach 1500 kPa, about 25 times of yield stress without compression.

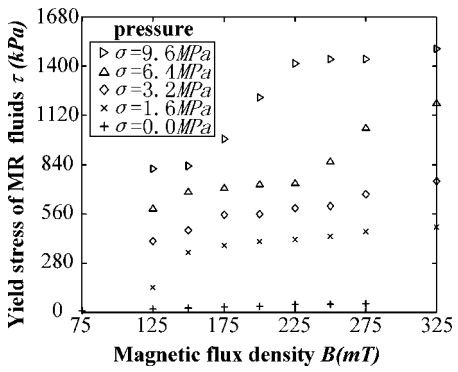

FIG. 5. 2D experimental results (measured by iron slice).

IV. PHYSICAL MODEL AND THEORETIC ANALYSIS

In this section, by considering both the local field theory employed in electrorheological (ER) fluids[7] and the friction during squeezing, a semiempirical model is developed to study the squeeze-strengthen effect.

A. Local field model

In a traditional dipole model, magnetizable particles are magnetized in a magnetic field and the magnetic force among the magnetic particles cause the MR effect, but only interaction between adjacent particles in the chain are considered. As such, by considering the interaction between all particles at the same chain, the dipole model is modified to study two cases of both before and after saturations.

1. Model before saturation

The magnetic field causes all particles in the chain to be induced. The field magnitude includes initial field and the induced magnetic field caused by these particles. Here a simple one-chain model is used while the influences of other chains are neglected.

When a magnetizable particle is placed in a magnetic field, its dipole moment is

$$\mathbf{m} = 3\mu_f\mu_0\beta V\mathbf{H}_{\text{loc}}, \tag{2}$$

where μ_0 is the vacuum permeability, $\beta=(\mu_p-\mu_f)/(\mu_p+2\mu_f)$, μ_p is the relative permeability of particles, and μ_f is the relative permeability of the medium, V is the volume of particle, $V=\frac{4}{3}\pi R^3$, and R is the radius of the particle. The local magnetic

$$\mathbf{H}_{\text{loc}} = \mathbf{H}_0 + \mathbf{H}_p, \tag{3}$$

where $\mathbf{H}_0$ is initial magnetic field and $\mathbf{H}_P$ is the magnetic field caused by dipole moment of particles in the chain. A dipole having moment of **m** will induce the magnetic field **H**

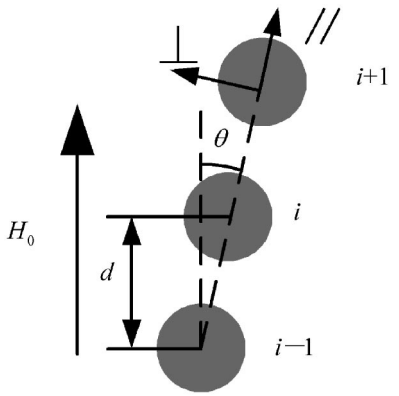

FIG. 7. Particles in a chain.

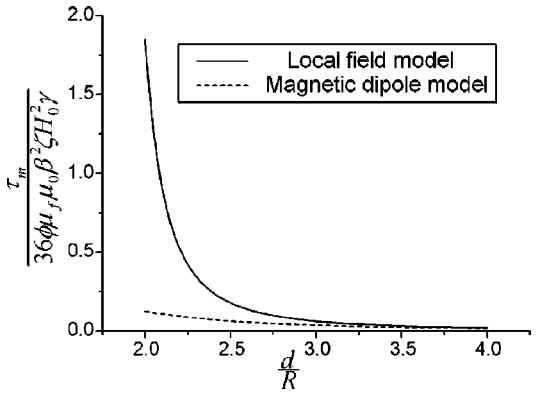

FIG. 8. Yield stress of modified dipole model (comparison with traditional dipole model).

$$\mathbf{H} = \frac{1}{4\pi\mu_f\mu_0 r^5}(-r^2\mathbf{m} + 3(\mathbf{m}\cdot\mathbf{r})\mathbf{r}), \tag{4}$$

where $r=|\mathbf{r}|$. As shown in Fig. 7, when the chain has a shear strain $\gamma=\tan\theta$ from its initial vertical direction (parallel to $\mathbf{H}_0$), the magnetic field in the center of the particle i caused by dipoles can be written as

$$H_{p,\parallel} = \frac{4\cos^3\theta m_\parallel}{4\pi\mu_f\mu_0 d^3}\sum_{k=1}^{\infty}\frac{1}{k^3} \tag{5}$$

and

$$H_{p,\perp} = -\frac{2\cos^3\theta m_\perp}{4\pi\mu_f\mu_0 d^3}\sum_{k=1}^{\infty}\frac{1}{k^3}, \tag{6}$$

Where d is the distance between two particles.

Combining Eqs. (2), (3), (5), and (6), $m_\parallel$ and $m_\perp$ are given by

$$m_\parallel = \frac{4\pi\mu_f\mu_0 R^3\beta H_0\cos\theta}{A}, \tag{7}$$

$$m_\perp = \frac{4\pi\mu_f\mu_0 R^3\beta H_0\sin\theta}{B}, \tag{8}$$

where $A=1-4\beta\cos^3\theta(R/d)^3\zeta$, $B=1+2\beta\cos^3\theta(R/d)^3\zeta$, $\zeta=\Sigma_{k=1}^{\infty}\frac{1}{k^3}\simeq 1.202$.

The interaction energy between particle i and other particles of the chain is

$$E = \frac{1}{4\pi\mu_f\mu_0}\left[\frac{2\zeta\cos^3\theta m_\perp^2}{d^3} - \frac{4\zeta\cos^3\theta m_\parallel^2}{d^3}\right]$$
$$= 4\pi\mu_f\mu_0\beta^2H_0^2\left(\frac{R^6}{d^3}\right)\cdot 2\zeta\cos^3\theta\left(\frac{\sin^2\theta}{B^2} - \frac{2\cos^2\theta}{A^2}\right). \tag{9}$$

Fluids with volume of V and particles volume fraction of ϕ have energy $E_t=(1/2\phi V/4/3\pi R^3)E$. The energy per unit volume is

$$E_d = E_t/V = (3\phi/8\pi R^3)E. \tag{10}$$

The shear stress induced by the application of a magnetic field can be calculated by taking the derivative of the energy density with respect to shear strain γ. Assume the shear deformation is small, the shear stress can be written as

$$\tau_m = 3\phi\mu_f\mu_0\beta^2H_0^2\left(\frac{R}{d}\right)^3\zeta\left(\left(\frac{10}{A^2}+\frac{2}{B^2}\right)\cos^6\theta\sin\theta + \frac{48\beta\zeta}{A^3}\left(\frac{R}{d}\right)^3\cos^9\theta\sin\theta\right). \tag{11}$$

For small shear strain, the additional shear stress approximation caused by the applied magnetic field can be obtained from Eq. (11),

$$\tau_m \approx 3\phi\mu_f\mu_0\beta^2H_0^2\left(\frac{R}{d}\right)^3\zeta\left(\left(\frac{10}{A^2}+\frac{2}{B^2}\right) + \frac{48\beta\varsigma}{A^3}\left(\frac{R}{d}\right)^3\right)\gamma. \tag{12}$$

Compare this equation with shear stress from traditional dipole model

$$\tau_m \approx 36\phi\mu_f\mu_0\beta^2H_0^2\left(\frac{R}{d}\right)^3\zeta\gamma. \tag{13}$$

If $R/d \ll \frac{1}{2}$ (i.e., the distance between particles is large), $A\to 1$ and $B\to 1$, Eq. (12) deteriorates for Eq. (13). It means that if the particles are not closed, the proposed model is compatible with the traditional dipole model. But if the particles are closed, according to Eq. (12), the shear stress increases sharply and cannot be neglected. A comparative figure of the local field model and traditional dipole model is shown in Fig. 8. When the particles become closed, deformation is sensitive on the magnetic field and the traditional dipole is no longer suitable. The shear stress increases sharply when the particles are packed. This result also indicates that if the MR fluids are compressed under a magnetic field, the MR effect becomes significant.

It should be noted that Eq. (12) is only valid for the single chain model where the influence of particles in other chains is neglected. For small volume fractions, this process is suitable. However, for large volume fractions, it is no longer valid, which is beyond the scope of this paper.

2. Model after saturation

When the magnetic field is large enough to make the particles attain saturation, Eq. (2) should be replaced by

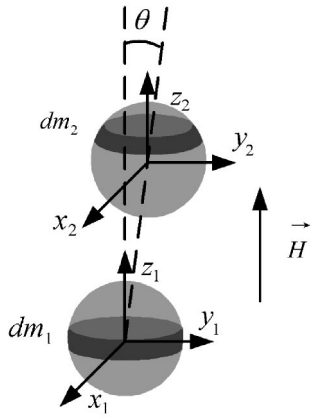

FIG. 9. Sketch map for energy calculation at saturation state.

$$\mathbf{m} = \mu_f \mu_0 \boldsymbol{M}_s V, \tag{14}$$

where $\mathbf{M}_S$ is the saturation magnetization. The additional shear stress caused by the dipole model is

$$\tau_{dm} = 4\phi\mu_f\mu_0 M_s^2 \left(\frac{R}{d}\right)^3 \gamma. \tag{15}$$

Traditional dipole model considered the particles to be a point in the center of the sphere. It is suitable only when the distance between particles is large. When the particles are closed, the model is modified by integrating the particles from many thin slices as shown in Fig. 9. The energy between two particles is

$$E = \int_{-R}^{R}\int_{-R}^{R} \frac{\cos^3\theta - 3\cos^5\theta}{4\pi\mu_f\mu_0(d + z_2 - z_1)^3} dm_1 dm_2, \tag{16}$$

where $dm_1 = \pi\mu_f\mu_0 M_s(R^2 - z_1^2)dz_1$, $dm_2 = \pi\mu_f\mu_0 M_s(R^2 - z_2^2)dz_2$.

A similar process is applied to Eq. (16), and the shear stress is obtained as Fig. 10. The vertical axis is the ratio of shear stress calculated by the proposed model with that of the traditional model. When the particles are far enough and the ratio is unity, two models are compatible. But when the particles touch each other in the chain, the shear stress is almost three times as much as the traditional dipole model. For example, if the carbonyl iron saturation is $\mu_0 M_s = 2.1T$, when the particles touch each other, from Fig. 10, then the shear stress of MR fluids can be $\tau_{sm} = 5.264\phi\gamma$ (MPa) before it reaches the yield point.

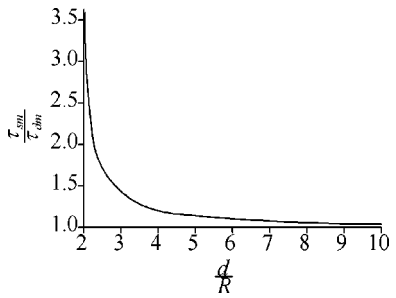

FIG. 10. Yield stress at saturation state by modified dipole model (comparison with traditional dipole model).

B. Tribology model

Tang *et al.*[5] have used Mohr–Coulomb theory to discuss the relationship of yield shear stress and normal stress. When the MR fluids are compressed, the influence of friction should be considered. If a magnetic particle contacts with a work piece, it will be deformed under the load.

In fact, when plastic deformation occurs because of heavy loading, contact area increases linearly with the load. This normal compression will be loaded on the contact area and produces friction. Usually magnetizable particles are covered by special surfactant and soaked in oil. When slip happens, only friction between the surfactant films occurs. When the film is broken, friction between the magnetizable particles happens. Suppose interfacial film has the shear strength τ_f, the particle material has the shear strength τ_0, the ratio C of τ_f and τ_0 should vary between 0 and 1. If the applied shear force is F_τ, when $F_\tau/A < \tau_f$, the junction area of the particles grow. When $F_\tau/A = \tau_f$, the films are broken and the junction area will disappear.

Based on the above analysis, the slide condition is $\sigma^2 + \alpha\tau_f^2 = \sigma_s^2$, where σ is the compression stress, $\alpha \approx \sigma_s^2/\tau_0^2$. Then $\sigma^2 + \alpha\tau_f^2 = \alpha\tau_0^2 = \sigma\tau_f^2/C^2$. So the relationship between the compression stress and the yield stress contributed by friction in MR fluids is

$$\tau_f = \frac{C}{[\alpha(1 - C^2)]^{1/2}}\sigma. \tag{17}$$

The factor in this formula is similar to $\tan\phi$ in Ref. 5, but here the influence of surfactant films has also been considered based on tribology theory.[8]

C. Synthetical model and result analysis

Combining above two considerations, the yield stress τ_y can be expressed as

$$\tau_y = K_1\tau_M + K_2\tau_f, \tag{18}$$

where τ_M is the yield stress of modified dipole model, τ_f is the yield stress by tribology, K_1 is contribution coefficient of τ_M and K_2 is contribution coefficient of τ_f, respectively. τ_M can be calculated by the modified dipole model [Eq. (19)]. But the state between unsaturated and saturated is too complex to be analyzed. To obtain the results between the before-saturation-state and the fully-saturation-state, a smoothing method is employed to interpolate values and to fit the surface between these two kinds of states. As such, a semi-empirical equation is given to express the yield stress τ_M at the general state,

$$\tau_M = \tau_{m\,\max} \times (1 - S) + \tau_{sm\,\max} \times S, \tag{19}$$

where $\tau_{m\,\max}$ is yield stress before saturation, it can be calculated from Sec. IV A 1 [Eq. (12)], and $\tau_{sm\,\max}$ is the yield stress after fully saturation, it can be calculated from Sec. IV A 2 (Fig. 10), S is a contribution factor, when $\tau_{m\,\max} \ll \tau_{sm\,\max}$, $S = 0$, and when $\tau_{m\,\max} \to \tau_{sm\,\max}$, $S \to 1$. When calculating $\tau_{m\,\max}$ and $\tau_{sm\,\max}$, the relation between the distance of particles and the compression stress σ loaded in the MR fluids is assumed as $R/d = 0.01\sigma + 0.4$.

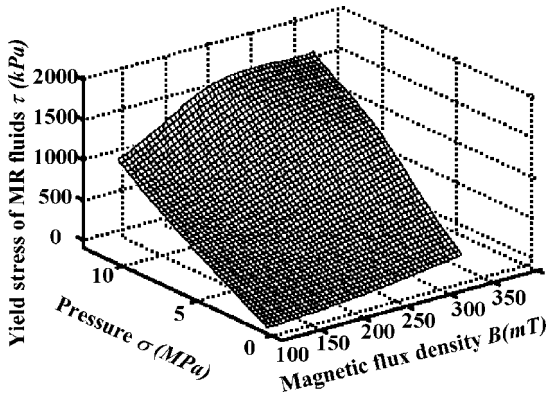

FIG. 11. Simulated yield stress from synthetical model (iron slice).

τ_f can be calculated according Sec. IV B [Eq. (17)]. Táng *et al.* have pointed out that the internal friction seems to increase slightly with the magnetic field. Here, its contribution coefficient is estimated empirically as

$$K_2 = \frac{1}{4}[\mathrm{sgn}(B - B_0)(1 - e^{(-|B-B_0|/\Delta)}) + 3],$$

where B_0 is the squeeze-strengthen effect critical magnetic flux density point, Δ is the intensity of strength changing. When the magnetic flux density and compression pressure reach critical extent, the construction is changed and the contribution of τ_f is enlarged consumedly.

By using Eq. (18), the yield stress of the experimental condition is simulated. When an iron slice is used to measure the stress, because an iron slice has higher permeability and strength, the squeeze-strengthen effect critical magnetic flux density point is low and C is high, we assume $B_0=50$ mT, $\Delta=20$ mT, $C=0.3$, $\alpha=9$. Because of the wall effects, the τ_M can be delivered entirely and we assume $K_1=1$. Thus the yield stress can be calculated and shown as in Fig. 11. When an aluminum slice is used to measure the stress, because aluminum slice has lower permeability and strength, the squeeze-strengthen effect critical magnetic flux density point is high and C is low, we assume $B_0=150$ mT, $\Delta=20$ mT, $C=0.1$, $\alpha=9$. Because aluminum slice has no wall effects, the τ_M cannot be delivered entirely and we assume $K_1=0.3$. Thus the yield stress can be calculated and shown as in Fig. 12. Comparing these two figures with the corresponding experimental results of Fig. 4 and 2, we can find that they show a similar outline.

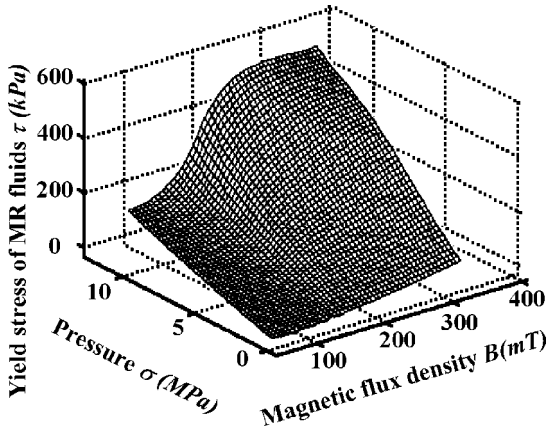

FIG. 12. Simulated yield stress from synthetical model (aluminum slice).

V. CONCLUSION

The squeeze-strengthen effect of MR fluids is experimentally and theoretically investigated. An apparatus is designed to experimentally study the effect and some promising results are obtained. For example, under the compression stress of 9.6 MPa, when magnetic flux density of 325 mT is applied on a MR fluid with volume fraction of 46%, the yield stress can reach 1500 kPa, 25 times of yield stress without compression. Such material is expected to meet wide industrial requirements, such as flexible fixture.

By considering the local field theory and the friction between the magnetizable particles, a semiempirical model is proposed to model this effect. The comparison between the simulation result and the experimental results indicates that this model can accurately predict the squeeze-strengthen effect.

This study also provides a good guidance to develop high-efficiency testing devices. To measure the large yield stress of MR fluids, test slice should be made of ferromagnetic materials such as iron. Because of the existence of the wall effect, when ferromagnetic material is used, binding between the test piece and fluid is strong, the fluid will be broken, then the measured stress really represents the yield stress of MR fluids. If a nonferromagnetic material such as an aluminum piece is used, binding between the test piece and fluid is weaker than that in MR fluids, then the measured stress only represents the binding between the test piece and MR fluids.

In addition, the proposed model may also be used to explain the squeeze-strengthen effect in ER fluids.[9]

ACKNOWLEDGMENTS

The authors want to thank S. Fang for his assistance and Dr. W.H. Li (University of Wollongong of Australia) for his help in English revisions. This research is supported by BRJH Project of Chinese Academy of Science and Specialized Research Fund for the Doctoral Program of Higher Education (No. 20030358014).

[1] M. Ginder, "Rheology Controlled By Magnetic Fields," *Encyclopedia of Applied Physies* (1996), Vol. 16, pp. 487–503.
[2] K. D. Weiss and T. G. Duclos, "Controllable fluids: The temperature dependence of post-yield properties," in *Proceedings of the 4th International Conference on ER Fluids, Singapore* (1994), pp. 43–59.
[3] J. M. Ginder and L. C. Davis, Appl. Phys. Lett. **65**, 3410 (1994).
[4] Y. Chen, H. Conrad, and X. Tang J. Intell. Mater. Syst. Struct. **7**, 517 (1996).
[5] X. Táng, X. Zhang, and R. Tao J. Appl. Phys. **87**, 2634 (2000).
[6] E. Lemaire and G. Bossis, J. Phys. D **24**, 1473 (1991).
[7] L. C. Davis, J. Appl. Phys. **72**, 1334 (1992).
[8] F. P. Bowden and D. Tabor, *The Friction and Lubrication of Solids* (Oxford University Press, Oxford, 1954).
[9] R. Tao, Y. C. Lan, and X. Xu, "Structure-enhanced yield stress in electrorheological fluids," in *Proceedings of the Eighth International Conference on Electrorheological Fluids and Magnetorheological Suspensions*, Nice, France, 2001, pp. 712–718.